

Investigations of Roughness Evolution in Uniaxial and Biaxial Stretching of Interstitial Free - IF Steel Sheet

José Divo Bressan^{1*}, and Ricardo Kirchoff Unfer¹

¹ Department of Mechanical Engineering, CCT, UDESC, CEP 89.219-710, Joinville, SC, Brazil

Abstract. The aim of work is to present experimental results for the evolution of surface roughness and waviness parameters with plastic strains in uniaxial and biaxial stretching tests of Interstitial Free-IF steel thin-sheet. Additionally, investigate the correlation between experimental FLC and Forming Limit Waviness curves of W_i^* , FLW, by displaying them on the same Map of Principal Surface Limit Strains, MPLS. Material plasticity parameters and strain hardening law were obtained by tensile tests at 0°, 45° and 90° to RD. Nakazima formability tests were performed using the Marciniak's flat head punch for in-plane stretching. Surface roughness and waviness profile parameters such as the maximum distance peak-valley roughness R_t , arithmetic average waviness W_a , total height peak-valley waviness W_t , maximum valley depth P_v were measured during uniaxial and biaxial tests. Nakazima uniaxial and biaxial samples were deformed in incremental steps to determine the negative and positive quadrants of the MPLS of IF steel. From these data, comparison of experimental and predicted local necking curve, FLC-N, by the strain gradient model, using Barlat's Yld 2000-2d yield function, and experimental FLW were plotted. Parameter W_i^* is nearly constant between 2.2 and 3.0 μm . Also, curves of roughness and waviness parameters versus equivalent strains were displayed.

Keywords: Roughness parameters; IF steel; Limit strains; Limit waviness curve.

1 Introduction

Sheet metal forming industries manufacture quality parts by shaping a thin metal blank in a press. Localized necking or fracture, rough surface appearance (orange peel) or high surface roughness are important topics of part failure and scrap problems. Thus, predictions of the limit strains and surface roughness in thin-sheet metal shaping operations are important issues in the process and mechanical analysis. The Map of Principal Surface Limit Strains, MPLS, which display the FLC curve of principal surface limit strains, are commonly used to assist the numerical simulation process in the part development phase. Thus, the MPLS is an important aid or "RoadMap" to the successful design of parts by thin-sheet metal forming numerical simulations. However, in engineering practice, information about the final surface roughness of the part in this "RoadMap" is not usually predicted or of concern in the part design and simulation phase. Nevertheless, surface roughness and waviness increase with plastic deformations and can reach unacceptable values in the different strain paths occurring in the deformed blank. Consequently, roughness and waviness parameters are very important surface quality parameters to be evaluated in sheet metal shaping. Roughness and waviness of sheet material plastically deformed are governed by various factors such as material plastic properties, the rolling process technique, the grain size, thickness and others.

Experimental and theoretical investigations on the increase of roughness parameter in sheet metal forming process have been performed and empirical mathematical expressions have been proposed in the literature, which correlate grain size, plastic strains and roughness parameters [1,2].

Fukuda et al. [1] have shown that the arithmetic average roughness parameter R_a of mild steel sheet increases linearly with the equivalent plastic strain, $R_a = R_{a_0} + k d_o \bar{\epsilon}$, where d_o is the average grain size, R_{a_0} is the initial arithmetic average roughness of sheet surface and k is a material constant. Yamaguchi and Mellor [2] have proposed a model based on Fukuda work to predict the limit strains, which linked the roughness parameter R_a to grain size and limit strains in sheet stretching of steel, aluminium and brass. The increase in surface roughness with plastic strain was shown dependent on the deformed material. The authors employed the M-K model to compute the limit strains, using the initial thickness defect parameter f calculated from the initial thickness t_0 and roughness parameter ($f = 1 - 2R_{a_0}/t_0$) and with the evolution of roughness according to Fukuda's equation. A similar approach by Stachowicz [3] proposed a model to predict the FLC of brass sheets, assuming that the growth of material defects depended on both the evolution of surface roughness parameter R_z and the growth of internal voids during the plastic deformation process. The author experimentally

* Corresponding author: josedivo.bressan@udesc.br

examined the limit strain curves of three different chemical compositions of brass sheet with four different grain size each. Stachowicz concluded that “The growth of surface roughness seems to be a more important factor that affected the level of the FLC than the inhomogeneity component caused by void growth, especially in the case of fine-grained materials.”

Bressan and Unfer [4] presented in 2015 an experimental work on the evolution of waviness and roughness parameters of IF steel sheet specimens of thickness 0.72 mm in uniaxial and biaxial stretching tests. Various waviness profile parameters were measured during uniaxial and biaxial tests such as the arithmetic average waviness Wa , the total height peak-valley waviness Wt , maximum peak height Pp and maximum valley depth Pv . The authors concluded that “The inception of visible local necking on the surface of deformed sheet metal in uniaxial tension and biaxial stretching tests can be monitored with high accuracy by the measurements of waviness parameters Wa and Wt . Local necking corresponds to a transition point of sharp increase in parameter Wa or Wt .” Furthermore, they observed that “The growth rate curves of waviness have shown that parameters Wa and Wt have initial tendency to stabilize with plastic deformation up to $\bar{\varepsilon} = 0.45$, a point well beyond the expected inception of plastic instability or diffuse necking calculated at $\bar{\varepsilon}_d = 0.25$.”

The objectives of present work are to model local necking from the onset of diffuse necking or instability [2]. Thus, revisit the concepts and mathematical models of diffuse necking which occurs before local necking in sheet metal forming. In addition, it aims to monitor the evolution of roughness and waviness parameters of IF steel sheet under experimental uniaxial tensile and biaxial stretching tests and confirm the tendency of waviness parameter to stabilize with plastic deformation under homogeneous straining process up to diffuse necking. The FLC-N curve is calculated to predict the inception of local necking, using the strain gradient approach proposed by Bressan et al. [5] from the initial diffuse necking point. Present work examines the formability of sheets through the comparative analysis of experimental results and theoretical modelling of the FLC-N under conditions of plane stress and linear strain paths. Also, measurements in the tensile and Nakazima tests were performed on the flat part of the specimen to enable roughness and waviness measurements and accurate measurements of surface strains.

2 Analysis of the Inception of Diffuse and Local Necking in Plane Stress

Local necking is preceded by diffuse necking in the forming of ductile sheet metals. Diffuse necking was firstly defined for tensile flat sheet specimen in uniaxial tension, occurring at the maximum load point condition. Before the maximum load point, the macroscopic plastic deformation process in the gauge part of specimen is considered homogeneous. Diffuse necking is an inhomogeneous strain distribution defined by a low strain gradient throughout the gauge part of specimen. However, microscopic shear bands or Lüders lines is

commonly observed in the specimen at the onset and evolution of plastic yielding in uniaxial tension tests.

2.1 Swift's diffuse necking

One first analysis of plastic instability at the inception of diffuse necking in sheet metal forming operations was presented by Swift [6]. The author assumed a thin-sheet under plane stress and drawing and biaxial stretching conditions (positive and negative quadrants of FLC). The onset of plastic instability or diffuse necking was defined to occur when simultaneous maximum loading is attained in the principal stress directions 1 and 2 in the sheet plane. Thus, considering a rectangular element of sheet metal under biaxial tension, the forces in the principal directions are $F_1 = A_1 \sigma_1$ and $F_2 = A_2 \sigma_2$, where A is the current cross section and σ_1 and σ_2 are the principal true stress. The Swift's condition for the onset of plastic instability was assumed to be when both loads simultaneously reach a maximum or the force increments are $dF_1 = 0$ and $dF_2 = 0$. Thus, the corresponding simultaneous mathematical differential equation which govern the beginning of plastic instability or the Swift's diffuse necking criterion is,

$$\frac{d\sigma_1}{\sigma_1} = d\varepsilon_1 \quad \text{and} \quad \frac{d\sigma_2}{\sigma_2} = d\varepsilon_2 \quad (1a,b)$$

where $d\varepsilon_1$ and $d\varepsilon_2$ are the principal plastic strain increments in the sheet plane.

Assuming the Barlat's Yld 2000 yield criterion Φ for plane stress [7] and the principal stress directions (1,2) coincident with the sheet orthonormal anisotropy axis (RD,TD), so the equivalent stress can be expressed as a function $\Phi(\sigma_1, \sigma_2) = \bar{\sigma}(\sigma_1, \sigma_2)$. Thus, from the total differential rule, the equivalent stress increment is: $d\bar{\sigma} = (\partial\bar{\sigma} / \partial\sigma_1) d\sigma_1 + (\partial\bar{\sigma} / \partial\sigma_2) d\sigma_2$. For constant principal stress ratio $X = \sigma_2 / \sigma_1$ and a_i the plastic anisotropy coefficients, the Barlat's Yld 2000-2d equivalent stress [8] can be expressed as $\bar{\sigma} = c \cdot \sigma_1$,

$$\bar{\sigma} = \left\{ \left[2^m |a_5 - a_6 X|^m + |a_1 + a_3 + (a_2 - a_4) X|^m \right] \right\}^{\frac{1}{m}} \frac{\sigma_1}{2^{1+1/m}} \quad (2)$$

Dividing both sides of the total differential of equivalent stress by $(\bar{\sigma})$, defining the strain path $\alpha = \partial\varepsilon_2 / \partial\varepsilon_1$, and for constant strain path and stress ratio $\partial\bar{\sigma} / \partial\sigma_1 = c$, thus $d\varepsilon_1 = d\lambda \cdot c$. Assuming the plastic potential function identical to the yield criterion, the strain increment definition for the plastic potential is $d\varepsilon_i = d\lambda (\partial\bar{\sigma} / \partial\sigma_i)$, rearranging and introducing the Swift's diffuse necking mathematical conditions of Eq. (1a,b) into the equivalent stress increment,

$$\frac{d\bar{\sigma}}{\bar{\sigma}} = \left(\frac{\partial\bar{\sigma}}{\partial\sigma_1} \right) \frac{d\sigma_1}{\bar{\sigma}} + \left(\frac{\partial\bar{\sigma}}{\partial\sigma_2} \right) \frac{d\sigma_2}{\bar{\sigma}} = [1 + \alpha^2 X] d\varepsilon_1 \quad (3)$$

Defining of equivalent strain increment as, $d\bar{\varepsilon} = Z_d d\varepsilon_1$, rearranging the Eq.3, the subtangent for the Swift's diffuse necking or instability condition is,

$$\frac{d\bar{\sigma}}{d\bar{\varepsilon}} = \frac{[1 + \alpha^2 X] \bar{\sigma}}{Z_d} = \frac{\bar{\sigma}}{Z_{Sw}} \quad (4)$$

Therefore, the Swift's diffuse necking or instability condition for $-0.5 \leq \alpha \leq 1$ is attained when,

$$Z_{Sw} = Z_d / [1 + \alpha^2 X] \quad (5)$$

Where Z_d is the subtangent at the instability condition of maximum principal major load in both the drawing or negative quadrant of forming limit diagram map, which is shown below.

2.2 Maximum principal load for diffuse necking

Another well-known plastic instability criterion for the onset of diffuse necking in sheet metal forming processes analysis is the condition of "maximum load point", where only the major force component $F_l = A_l \sigma_l$ is maximum in the sheet plane. Thus, the differential equation that govern the beginning of plastic instability for constant stress ratio X or strain path α is,

$$\frac{d\sigma_1}{\sigma_1} = \frac{d\bar{\sigma}}{\bar{\sigma}} = d\varepsilon_1 \quad (6)$$

Defining the subtangent for diffuse necking at the point of maximum load $d\bar{\sigma} / d\bar{\varepsilon} = \bar{\sigma} / Z_d$, and the increment of equivalent strain, $d\bar{\varepsilon} = Z_d d\varepsilon_1$, in the range $-0.5 \leq \alpha \leq 1$, thus,

$$\frac{d\bar{\sigma}}{d\bar{\varepsilon}} = \frac{\bar{\sigma}}{Z_d} \quad (7)$$

and from the definition of plastic work increment for plane stress, $dw = \bar{\sigma} d\bar{\varepsilon} = \sigma_1 d\varepsilon_1 + \sigma_2 d\varepsilon_2$, the increment of equivalent strain is, $d\bar{\varepsilon} = (\sigma_1 / \bar{\sigma})(1 + \alpha X) d\varepsilon_1$. Therefore, the subtangent Z_d is,

$$Z_d = (\sigma_1 / \bar{\sigma})(1 + \alpha X) \quad (8)$$

2.3 Hill's local necking

Hill [9] proposed the following differential equation or criterion for the onset of local necking in the negative quadrant of MPLS map in sheet metal forming operations,

$$\frac{d\sigma_n}{\sigma_n} = \frac{d\bar{\sigma}}{\bar{\sigma}} = -d\varepsilon_3 \quad (9)$$

where σ_n is the stress component perpendicular to the direction along the neck, which is of zero extension in

the sheet plane, and $d\varepsilon_3$ is the thickness strain increment. Considering volume constant, Eq. 9 can be rewritten as,

$$\frac{d\bar{\sigma}}{\bar{\sigma}} = (1 + \alpha) d\varepsilon_1 = (1 + \alpha) \frac{d\bar{\varepsilon}}{Z_d} \quad (10)$$

Consequently, the Hill's local necking condition is the subtangent $Z_{Hill} = Z_d / (1 + \alpha)$, for the strain paths in the negative quadrant of the MPLS map or for uniaxial test $\leq \alpha \leq$ plane strain.

2.4 Strain gradient approach to predict local necking, FLC-N

Modelling the prediction of FLC curve have been presented by different approaches on the mechanics of local necking origin and evolution: the M-K model [10] of initial thickness imperfection and the model of arising a vertex on the subsequent yield surface [11]. Subsequently, Bressan and Williams [5] proposed an alternative approach for the inception of local necking, based on the concept of plastic strain gradient evolution from an initial thickness defect. The strain gradient was defined as the derivative $\lambda = \partial \bar{\varepsilon} / \partial x$, where x is the coordinate axis perpendicular to the groove. The initial thickness defect was $\mu = (1 / A_o) dA_o / dx$, where A_o is the initial thickness area of the thickness cross section in the groove or neck. The plastic strain gradient evolution model considers a continuous grows of localized strain gradient from the largest initial thickness defect that culminates with a visible localized necking or groove or narrow surface band and the subsequent rupture. When the local strain gradient λ reaches a critical value of about 20 (1/mm) or when the normalized strain gradient $\lambda / \mu = (\lambda / \mu)^*$ is a constant, a macroscopic visible local necking arises in the initial thickness defect site. Thus, the prediction of the FLC-N curve of local necking in the MPLS map can be calculated for the different strain paths. The following differential equations which govern creation and growth of localized strain gradient until very close to a visible local necking in thin sheet deformed in the negative ($-0.5 \leq \alpha \leq 0$) and positive quadrant ($1 \leq \alpha \leq 0$) of MPLS map, for a strain and strain rate hardening material are respectively Eqs. 11 and 12 which describes the FLC-N [12],

$$\frac{\partial(\lambda / \mu)}{\partial \bar{\varepsilon}} = \frac{1}{M} + \frac{1}{M} \left\{ \frac{1}{Z_{Hill}} - \frac{n}{(\varepsilon_o + \bar{\varepsilon})} \right\} \frac{\lambda}{\mu} \quad (11)$$

$$\frac{\partial(\lambda / \mu)}{\partial \bar{\varepsilon}} = \frac{1}{M} + \frac{1}{M} \left\{ \frac{1}{Z_d} - \frac{n}{(\varepsilon_o + \bar{\varepsilon})} \right\} \frac{\lambda}{\mu} \quad (12)$$

where the parameters n and M are the exponents of the strain and strain rate hardening material which equivalent stress is $\bar{\sigma} = K (\varepsilon_o + \bar{\varepsilon})^n (\dot{\bar{\varepsilon}} / \dot{\varepsilon}_o)^M$, the pre-strain is ε_o and $(\dot{\bar{\varepsilon}} / \dot{\varepsilon}_o)$ the normalized strain rate. Therefore, Eq. 11 and Eq. 12 have to be numerically

integrated from the initial equivalent true plastic strain $\bar{\epsilon} = 0$ or $\bar{\epsilon} = \bar{\epsilon}_o$ up to a critical limit strain $\bar{\epsilon} = \bar{\epsilon}_{cr}$ when $(\lambda/\mu)^*$ reaches a critical value.

Alternatively, assuming uniform macroscopic plastic strain up to maximum loads point (Swift or maximum principal major load) conditions and linear strain path, the limit of equivalent plastic strain at local necking can be calculated from the beginning of equivalent true strain $\bar{\epsilon} = \bar{\epsilon}_{diffuse} = Z_{diffuse} n - \epsilon_o$ up to the limit strain $\bar{\epsilon} = \bar{\epsilon}^*$, where the subtangent $Z_{diffuse}$ could be Z_{Sw} or Z_d . Consequently, for linear strain path, $\bar{\epsilon} = z_d \epsilon_1$, the total major true plastic strain ϵ_1^* at the onset of visible surface local necking or the FLC-N can be calculated as the sum of the instability strain and the subsequent strain up to local necking by,

$$\epsilon_1^* = \epsilon_{1d} + \epsilon_{1pi} = \frac{Z_{diffuse}}{Z_d} n - \frac{\epsilon_o}{Z_d} + \epsilon_{1pi} \quad (13)$$

where the post instability major limit strain ϵ_{1pi} is calculated by integrating Eq. 11 and Eq. 12.

3 Material and Experimental Procedure

The formability tests of IF steel sheets were performed by tensile and Nakazima test specimens. Tensile and biaxial stretching specimens were manufactured by laser cutting from cold rolled interstitial free steel-IF sheets with thickness of 0.82 mm, provided by the Brazilian company Arcelor Mittal, Vega do Sul, São Francisco do Sul, SC, Brazil. The tensile specimens were cut at the directions of 0°, 45° and 90° relative to the rolling direction (*RD*) and tested as received at strain rates of 0.072s⁻¹ and 0.78s⁻¹ and at room temperature. The simple tensile specimens had geometry according to the JIS-Z-2241-1998 standard which had width of 25 mm. The obtained average mechanical plastic properties of IF steel specimens are shown in Table 1, using 3 specimens for each test condition. The Swift modified strain and strain rate hardening law obtained in uniaxial tensile tests was $\sigma = 572.4 (\epsilon_o + \epsilon)^{0.290} \dot{\epsilon}^{0.014}$ [MPa].

The Nakazima biaxial stretching specimens were manufactured by laser cutting and had geometry of flat discs or strips cut from discs of 220 mm in diameter. The specimens had appropriate gauge length of 50 mm and gauge width to attain uniaxial tensile (60 mm), plane strain (135 mm), biaxial intermediary (150 and 170 mm) and balanced biaxial (220 mm). The stretching strain paths in the stretching and drawing quadrants of MPLS map was performed, using the Marciniak's flat head punch of 100 mm and double blank [10] in the deformation process with the major surface strain aligned 0° to *RD*. The auxiliary blank had thickness of 2 mm and a central hole of 34 mm to produce the in-plane uniaxial and biaxial tension tests. A grid of circles of 2.50 mm was printed on the specimen surface and the major and minor principal surface strains were measured in the central region of the flat surface of specimen. The linear plastic strain paths were performed

incrementally with intermediate stops to allow measurements of principal plastic strains and the surface roughness and waviness parameters. The punch displacement at each step was about 2 mm and velocity of 1 mm/min. Measurements of these parameters on the specimen flat surface was carried out in 3 points in the specimen centre region, and repetitions of 3 specimens for each test condition or strain path, using a roughness meter of high accuracy of 0.01 µm, Talysurf 25, cutoff 4 mm. The initial average roughness of specimens was $Ra = 1.00$ µm, maximum distance peak-valley $Rt = 6.67$ µm, the average waviness parameters $Wa = 0.70$ µm, waviness maximum distance of peak-valley $Wt = 3.18$ µm and maximum valley depth was $Pv = 4.55$ (µm).

Initially, the measurement for each deformation step in uniaxial tension tests, the recorded elongation length of each specimen was about 2 mm. The displacement step was then reduced to 1 mm when the specimen reached maximum load until the onset of local necking. For plane strain and biaxial stretching specimens using the flat punch, the punch displacement at each step was about 2 mm. After each plastic strain step, measurements were made on the printed circle grid in order to obtain the values of principal strains on the specimen surface, using a profile projector accurate to 1 µm. It was also performed the measurement of roughness and waviness parameters on the specimen surface at 3 points in the central region of specimen, with Talysurf 25. The measurements were taken inside the expected site of localized necking. The following roughness parameters were considered: arithmetic average roughness Ra (µm), maximum distance peak-valley Rt (µm); and waviness parameters such as arithmetic average waviness Wa (µm), total height of peak-valley waviness Wt (µm) and maximum valley depth Pv (µm). From the experimental step points obtained in the formability tests, it was possible to plot the curves of roughness and waviness parameters measured at 0° and 90° to the rolling direction, *RD*, versus the equivalent plastic strain of IF steel for the Nakazima sheet specimens.

4 Results and Discussions

The evolution of roughness and waviness parameters are in seen Fig. 1 - 3, but truncated for large values. In Fig. 1, the experimental results of growth of the arithmetic average of waviness Wa with the increase of plastic equivalent strain during the Nakazima formability tests of IF steel sheet specimens are shown up to local necking (Wa at necking is truncated). It is observed that the parameter Wa is approximately linear, but constant at $Wa = 1.5$ µm up to the equivalent plastic strain of about $\bar{\epsilon} = 0.22$. Thus, the waviness parameter Wa is initially 0.70 µm and remains approximately constant from $\bar{\epsilon} = 0.08$ up to $\bar{\epsilon} = 0.22$, which correspond to the point of beginning of diffuse necking. Sharp increase in parameter Wa occurs between $Wa = 3.4$ and 4.0 µm, which correspond to the inception of local necking, but for different equivalent plastic strains. Additionally, in Fig. 2, the parameters roughness maximum distance peak-valley Rt and the total height peak-valley of

Table 1. Mechanical plastic properties of measured IF steel specimens. Tensile tests performed at strain rates of $0.072s^{-1}$ and $0.78s^{-1}$ and at room temperature.

Coefficient of anisotropy r			Coeff. biaxial	Yield stress limit [MPa]			Strain hardening exponent n			Strain rate hardening exponent M			pre-strain ϵ_0
r_0	r_{45}	r_{90}	r_b	σ_0	σ_{45}	σ_{90}	n_0	n_{45}	n_{90}	M_0	M_{45}	M_{90}	ϵ_0
2.31	2.05	2.81	0.996	134	181	137	0.290	0.215	0.276	0.012	0.011	0.018	0.0063

Obs. The calculated balanced biaxial yield stress was $\sigma_b = 179$ MPa (calculated according to Hill 48).

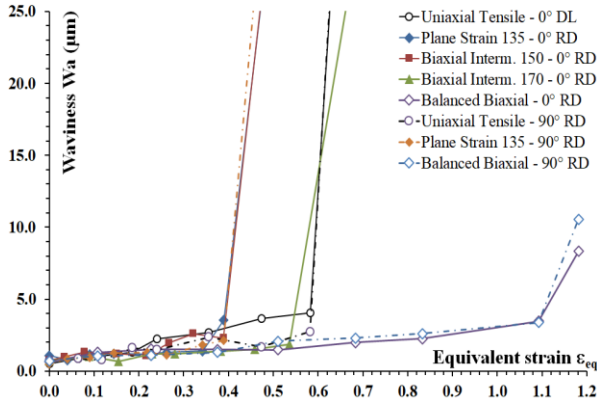


Fig. 1 Experimental growth of the arithmetic average of waviness Wa versus the equivalent plastic strain for the different strain paths from the Nakazima formability tests of IF steel sheet.

waviness Wt are displayed. The parameter Rt had very low growth up to point $\bar{\epsilon} = 0.24$ of diffuse necking.

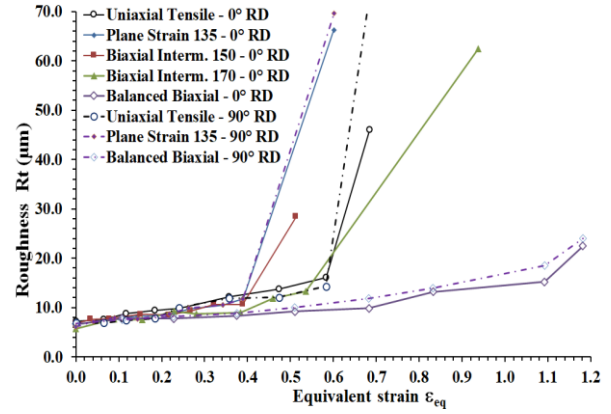
Overall, the growth of roughness parameter Rt is approximately linear, but a sharp increase in the roughness parameter Rt occurs between $Rt = 14$ and $15 \mu m$, which correspond to the point of inception of localized necking. However, the waviness parameter of total height peak-valley Wt presented similar tendency, but greater variations with the different strain paths.

The growth of waviness parameter of maximum valley depth Pv is also overall linear with the equivalent strain as seen in Fig. 3. However, at the initial plastic deformation stages up to about $\bar{\epsilon} = 0.20$ of diffuse necking, the parameter Pv is also approximately constant or very low growth for each strain path. The limit of Pv before the sharp increase near local necking is circa $14 \mu m$.

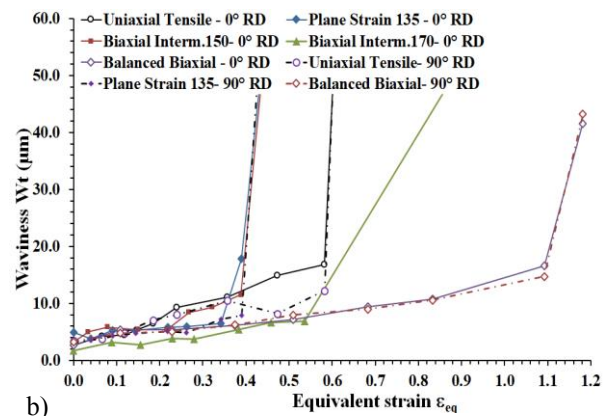
In Fig. 4, the calibration of the Barlat's Yld 2000-2d yield stress and the associated plastic stress potential with the experimental results, for exponent $m=6$, are shown. The recommended experimental calibration parameters, 4 s-values and 4 r-values, were: $\sigma_0, \sigma_{45}, \sigma_{90}, \sigma_b, r_0, r_{45}, r_{90}, r_b$, according to Table 1. The inflection point at 45° was not expected, r_{30} was not available.

The calculated plastic anisotropy coefficients a_i of the Barlat Yld 2000-2d yield stress and the correspondent associated plastic potential are seen in Table 2. The predicted biaxial plastic parameters, using the equations in [8], were $r_b = 0.995$ and $\sigma_b = 1.336 \times 134 = 179.0$ MPa, which are identical to the experimental values seen in Table 1.

The analysis of the predicted FLC-N curves, using the evolution of local strain gradient from the beginning of diffuse necking models are shown in Fig. 5.



a)



b)

Fig. 2 Experimental growth of the roughness and waviness parameters versus the equivalent plastic strain for the different strain paths from Nakazima formability tests of IF steel sheet: a) roughness of maximum distance peak-valley Rt and b) waviness of total height of peak-valley Wt .

Table 2. The calculated plastic anisotropy coefficients of the Barlat Yld 2000-2d yield stress criterion $\Phi(\sigma_{ij}, a_i)$ and associated plastic stress potential of IF steel, exponent $m=6$.

Experim.	a_1	a_2	a_3	a_4
	0.857503	0.637940	1.096885	1.126002
$\Phi: 4s+4r$	a_5	a_6	a_7	a_8
	1.020468	1.042563	0.783745	0.610321

The MPLS map with the predicted FLC-N curves for the strain gradient approaches and the fitting with the experimental results of IF steel sheets from the Nakazima formability tests, and also the pure shear tests, are presented in Fig. 5.

Two strain gradient models applied from diffuse necking were considered to calculate the major principal surface limit strain, according to Eq. 13.

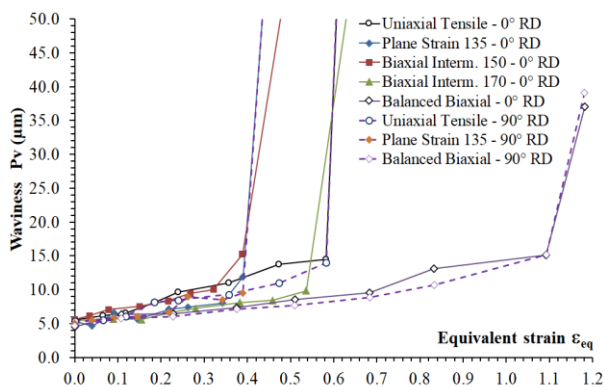


Fig. 3 Experimental growth of the maximum valley depth of waviness P_v vs equivalent plastic strain for the different strain paths from the Nakazima formability tests of IF steel sheet.

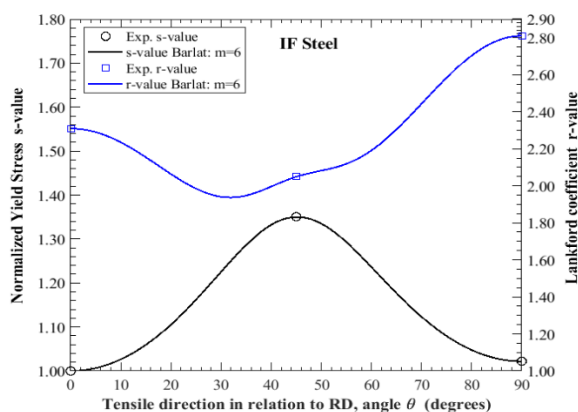


Fig. 4 Fitting of the predicted r-value and s-value curves of Barlat's Yld 2000-2d yield stress and associated plastic potential with the experimental results of IF steel, exponent $m=6$, using experimental calibration parameters: 4 s-values and 4 r-values: $\sigma_0, \sigma_{45}, \sigma_{90}, \sigma_b, r_0, r_{45}, r_{90}, r_b$.

First, the normalized strain gradient λ/μ grows from the beginning of Swift's diffuse necking, Eq. 5; and second, the strain gradient grows from the beginning of point of maximum major load for diffuse necking, Eq. 8. Visible localized necking was assumed to occur when the strain gradient reach $\lambda/\mu = 1.8$ from the beginning of Swift's diffuse necking, and from the beginning of maximum major load diffuse necking when the strain gradient reach $\lambda/\mu = 1.7$. The results show that the approach which assumes the evolution of the strain gradient λ/μ from the beginning of Swift's diffuse necking had better fitting with the experimental local necking limit, FLC-N. Furthermore, the waviness parameters limit of peak-valley W_t^* and the valley depth P_v , the waviness limit curves named FLW, near the local necking are also displayed. The parameter W_t^* is approximately constant between 2.2 and 3.0 μm , P_v is nearly constant at 14 μm .

5 Conclusions

From the analysis of experimental results on local necking curves, roughness and waviness parameters from uniaxial and biaxial stretching in Nakazima tests of ductile IF steel sheet deformed up to rupture, the following main conclusions can be summarized:

a) Inception of visible local necking on the surface of sheet metal in uniaxial and biaxial stretching tests can

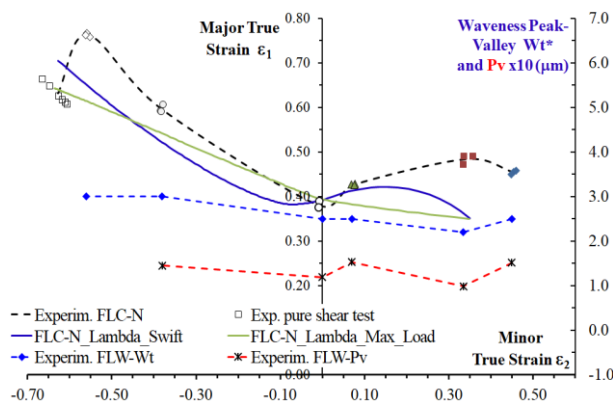


Fig. 5 MPLS map with the predicted FLC-N curve fitting with the experimental results of IF steel sheets from Nakazima formability tests and pure shear tests. The limit curves of waviness of peak-valley W_t^* and the valley depth P_v , FLW, near the local necking are also displayed.

be monitored with high accuracy by the measurements of the waviness parameters: height of peak-valley W_t and maximum valley depth P_v . Local neck corresponds to sharp transition point in the growth curve of W_t or P_v . b) Growth of the parameters average of waviness W_a , height of peak-valley W_t and maximum valley depth P_v is overall linear with equivalent strain. However, at the initial plastic deformation stages up to about $\bar{\epsilon} = 0.22$, which is the point of onset of diffuse necking, the parameters W_a , W_t and P_v are almost constant or very low growth in each strain path. Thus, the approach which assumes evolution of strain gradient λ/μ from the beginning of Swift's diffuse necking had better fitting with the experimental FLC-N.

c) The waviness limit curves, FLW, near the local necking were also displayed. The limit waviness parameter W_t^* is approximately constant between 2.2 and 3.0 μm and the limit P_v is nearly constant at 14 μm .

Acknowledgements

The authors would like to gratefully thank CNPq of Brazil; Arcelor Mittal, São Francisco do Sul, SC, Brazil, for the specimens and the University - UDESC, Brazil.

References

1. M. Fukuda, K. Yamaguchi, N. Takakura, Y. Sakano. J. Japan Soc. Tech. Plasticity, **15** (1974)
2. K. Yamaguchi and P.B. Mellor. Int. J. Mech. Sci., **18** (1976)
3. F. Stachowicz. Acta Mech., **227** (2016)
4. J.D. Bressan and R.K. Unfer. Key Engineering Materials, v. **651-653** (2015)
5. J.D. Bressan and J.A. Williams. J. Mech. Working Tech., **11** (1985)
6. H.W Swift. J. Mech. Phys. Solid, **1**, 1 (1952)
7. F. Barlat, J.C. Brem, J.W. Yoon, K. Chung, R.E. Dick, D.J. Lege, F. Pourboghra, S.-H. Choi and E. Chu. Int. J. Plast., **19** (2003)
8. J.D. Bressan and M.V. Donadon. J. Mater. Eng. Perform., ASTM, online March/2023 (2023)
9. R. Hill. J. Mech. Phys. Solids, **1** (1952)
10. Z. Marciniak, K. Kuczynski, T. Pokora. Int. J. Mech. Sci., **15** (1973)
11. S. Stören, J.R. Rice. J. Mech. Phys. Solids, **23** (1975)
12. J.D. Bressan, S. Bruschi and A. Ghiotti. Int. J. Mech. Sci., **115-116** (2016)